Lifelong molecular consequences of high Glucocorticoids exposure during development

Min-Kyeung Choi[1], Alex Cook[2], Kanak Mungikar[2], Helen Eachus[1], Anna Tochwin[1], Matthias Linke[2], Susanne Gerber[2], Soojin Ryu[1]*

[1] Living Systems Institute, Faculty of Health and Life Sciences, University of Exeter, Stocker Road, Exeter, EX4 4QD, United Kingdom

[2] Institute of Human Genetics, University Medical Center, Johannes Gutenberg University Mainz, Langenbeckstraße 1, 55131, Mainz, Germany

* Correspondence: s.ryu@exeter.ac.uk

Keywords: Stress, Zebrafish, Brain, Glucocorticoids, Epigenetics

Running Title: Zebrafish Glucocorticoid Primed Genes

Abstract

Early life stress (ELS) is one of the strongest risk factors for developing psychiatric disorders in humans. As conserved key stress hormones of vertebrates, glucocorticoids (GCs) are thought to play an important role in mediating the effects of ELS exposure in shaping adult phenotypes. In this process, early exposure to high level of GCs may induce molecular changes that alter developmental trajectory of an animal and primes differential adult responses. However, comprehensive characterization of identities of molecules that are targeted by developmental GC exposure is currently lacking. In our study, we describe lifelong molecular consequences of high level of developmental GC exposure using an optogenetic zebrafish model. First, we developed a new double-hit stress model using zebrafish by combining exposure to a high endogenous GC level during development and acute adulthood stress exposure. Our results establish that similar to ELS-exposed humans and rodents, developmental GC exposed zebrafish model shows altered behavior and stress hypersensitivity in adulthood. Second, we generated time-series gene expression profiles of the brains in larvae, in adult, and upon stress exposure to identify molecular alterations induced by high developmental GC exposure at different developmental stages. Third, we identify a set of GC-primed genes that show altered expression upon acute stress exposure only in animals exposed to a high developmental GC. Interestingly, our datasets of GC primed genes are enriched in risk factors identified for human psychiatric disorders. Lastly, we identify potential epigenetic regulatory elements and associated post-transcriptional modifications following high developmental GC exposure. Thus, we present a translationally relevant zebrafish model for studying stress hypersensitivity and alteration of behavior induced by exposure to elevated GC levels during development. Our study provides comprehensive datasets delineating potential molecular targets underlying the impact of developmental high GC exposure on adult responses.

Introduction

Early life stress (ELS) affects healthy development and aging as well as susceptibility to psychiatric disorders in humans[1-4]. Studies in humans and animals suggest ELS may increase risk for psychiatric diseases such as depression by inducing hypersensitivity to future stress exposure[5-8]. However, mechanism by which ELS sensitizes responses to future stress responses in adulthood remains poorly understood. In vertebrates, stress response is mediated by a highly conserved neuroendocrine system called the Hypothalamic-Pituitary-Adrenal axis (HPA-axis) in humans[9] and the Hypothalamic-Pituitary-Interrenal axis (HPI-axis) in fish whose activation result in the release of Glucocorticoids (GCs)[10]. While GCs have pleiotropic effects on many

aspects of animal physiology, exposure to elevated GCs during brain development is known to cause long-term alteration of behavior, physiology, and stress regulation[11]. However, how exposure to high levels of GC during development predisposes individuals to adulthood dysfunction is poorly understood. One potential mechanism is long-lasting epigenetic changes, which modify how animals respond to stress in adulthood[12]. For example, altered DNA methylation at the glucocorticoid receptor (GR) gene promoter induced by poor maternal care is associated with adulthood alterations in histone acetylation, DNA methylation, transcription factor binding, GR expression, and the HPA response to stress[13]. Moreover, a recent study identified differentially expressed genes (DEGs) "primed" by ELS in specific regions of ELS-exposed mouse brains[14]. These genes showed enhanced differential expression in ELS-exposed animals in adulthood upon re-exposure to stress and may be associated with behavioral changes in adulthood. Another study identified direct GC-primed DEGs and associated long-lasting DNA methylation alterations using a GC (dexamethasone)-exposed human hippocampal progenitor cell line[15]. Together, the above studies establish that ELS or developmental GC exposure results in distinct responses to stress later in life by priming and maintaining longer-term alteration of specific genes. However, so far, ELS- or GC-primed genes have only been identified in specific regions of the brain including reward circuitry or specific cell lines, and brain-wide GC-primed molecular alterations have not been investigated.

Here we report whole brain transcriptomic alterations of high GC-exposed fish across the life course and upon acute stress exposure in adulthood. Interestingly, when subjected to acute stress in adulthood, developmental high GC-exposed fish show highly exaggerated endocrine and transcriptional responses, indicating that adult stress is processed differently depending on the GC exposure history of an animal. The genes primed by developmental GC-exposure were enriched in gene sets associated with human neuropsychiatric disorders, suggesting similarity of molecular mechanisms by which early GC exposure leads to altered adult functions among vertebrates. We identify hitherto uncharacterized novel GC-primed genes that are enriched in synapse and neuronal signaling function. Whole brain DNA methylation analysis identified some of them as direct targets of developmental GC-mediated epigenetic modifications. Lastly, the expression of many epigenetic modulators affecting RNA processing, histone modification and DNA modification are altered following acute stress in developmental GC-exposed individuals, which can contribute to the different physiological and behavioral responses following adult stress exposure in later stage of life.

Results

87 **Double-hit zebrafish stress model exhibit altered adulthood stress response**
88 We developed a double-hit stress model using zebrafish which combines exposure to a high
89 level of GC during development with acute adult stress exposure (Fig. 1a). Firstly, we used our
90 previously reported optogenetic transgenic model *Tg(star:bPAC-2A-tdTomato)* where the
91 elevation of endogenous cortisol (GC in fish) is induced by blue light which activates *beggiatoa*
92 Photoactivated Adenylyl Cyclase (bPAC), expressed specifically in steroidogenic interrenal
93 cells[16-18] (Fig. 1b). Like the mammalian adrenal gland, the fish interrenal gland is composed of
94 two cell types: aminergic chromaffin cells and steroidogenic interrenal cells, the latter of which
95 produce glucocorticoids (GCs). We established that *Tg(star:bPAC-2A-tdTomato)*^{uex300} raised
96 under ambient light containing blue light (hitherto referred to as bPAC+) showed increased
97 cortisol level and expression of *fkbp5*, one of known GR signaling marker genes[19,20], at larval
98 stages[17,18] (Fig. 1c). Elevated cortisol levels through larval and juvenile stages were detected
99 in bPAC+, but not maintained until adulthood (after 3 months) allowing us to achieve a robust
100 and persistent increase in endogenous cortisol levels during development (Fig. 1d-e).
101 Throughout the study, bPAC+ fish were compared to bPAC-, siblings of bPAC+ which do not
102 carry the transgene themselves but are offspring of a bPAC+ parent crossed to wild type. We
103 also compare their phenotypes to wildtype TU, which is the same strain as bPAC+ and bPAC-,
104 to determine possible effects resulting from elevated GC in parental generation (S. Fig. 1).
105 Secondly, for acute stress delivery, we utilized a looming dot stimulus (LD), which mimics an
106 approaching predator[21] (Fig. 1f). bPAC+ adults exhibited an exaggerated endocrine response
107 after LD exposure compared to wildtype or bPAC- adults and even an elevated GC level
108 induced by handling before the LD exposure (Fig. 1g), indicative of a highly sensitized
109 endocrine response to acute stress in bPAC+.
110
111 **High GC-exposed animals during development show altered behaviors in adulthood**
112 To determine whether exposure to a high level of endogenous GC during development (dGC)
113 alters adult functions, we tested adult behavior encompassing different behavioral domains
114 using wildtype, bPAC- and bPAC+ (Fig. 2). We first established that they did not show
115 significant differences in basal locomotor activity (Fig. 2b-c). We then used a novel tank test
116 to assess their adaptive responses in a novel environment[22,23] (Fig. 2d-g). When placed in a
117 novel tank, zebrafish typically first dive to the bottom whilst performing bouts of erratic high-
118 speed swimming[22,23]. There was no significant difference between bPAC- and wildtypes in
119 average depth or fast swimming time (Fig. 2e, g). In contrast, bPAC+ fish showed reduced
120 depth-preference (Fig. 2e) and reduced fast-swimming compared to bPAC- and wildtype fish

121 (Fig. 2g). In addition, bPAC+ showed reduced average speed compared to wild type (Fig. 2f).
122 Next, we tested feeding behavior by counting the number of floating food pellets eaten by a
123 fish during a 10-minute interval (Fig. 2h). Wild-type and bPAC- adult fish consumed on
124 average 14.5 and 11.25 pellets, respectively while bPAC+ fish consumed significantly fewer
125 pellets (on average 2.33 pellets out of 25) (Fig. 2i-j). This was not due to the lack of recognition
126 nor interest in the food, as bPAC+ fish approached the food pellets and spent a longer time
127 near the pellets (feeding zone) than bPAC- and wildtype fish (Fig. 2k). Further, we analyzed
128 social behavior using a new test that we recently established, which allows measuring both
129 social approach and social interaction within a same paradigm (Fig. 2l). While bPAC+
130 exhibited reduced social interactions compared to wild type, no significant difference was
131 observed in bPAC+ compared to bPAC- (Fig. 2m-o). Similarly, whilst bPAC+ exhibited
132 altered fear conditioning behavior compared to wildtype, there was no significant difference
133 observed between bPAC+ and bPAC- in an associative learning test using a Pavlovian
134 avoidance learning test[24,25] (Fig. 2p-s). Thus, exposure to a high level of endogenous GC during
135 development led to an exaggerated endocrine response upon acute stress exposure in adulthood
136 and alteration in responses in novel environment and feeding behaviors. For social and fear
137 conditioning behaviors, exposure to a high GC during parental generation appear to be
138 sufficient to modify adult behavior.
139
140 **Distinct transcriptional alterations in bPAC+ fish across the life course**
141 To identify transcriptional changes caused by dGC-exposure, we performed time series whole-
142 brain RNA sequencing using larval (6 and 13 dpf) and female adult (120 dpf) brains of bPAC+,
143 bPAC-, and wildtype fish. The total number of DEGs identified among different genotypes
144 varied starkly at different time points. The global gene expression profiles of bPAC+ were
145 clearly distinct from those of wild types while bPAC- profiles mapped more closely to those
146 of bPAC+ than wild type (S. Fig. 2a). The overall expression pattern of identified DEGs using
147 the threshold (FDR < 0.05 and $|\log_2(\text{fold-change, FC})| > 1.5$, S. Data File 1) mainly exhibited
148 a close grouping primarily based on groups and time point except for two 13 dpf bPAC- profiles
149 (Fig. 2a).
150 In bPAC+ and bPAC- comparisons which reveal alterations induced by dGC-exposure, a large
151 number of DEGs were identified at the early larval stage (6 dpf, up/downregulated DEGs:
152 1147/1631), but a much fewer number of DEGs were detected at 13 dpf (28/79) and 120 dpf
153 (47/278). At 6 dpf, we observed transcriptional alterations of genes that are previously reported
154 to be altered following GC treatment, including *fkbp5*[19,20] and *hsd11b2*[26] (Fig. 3b). In the adult

155 bPAC+ brains, 27% (13 genes) of the upregulated and 31% (88 genes) of the downregulated
156 DEGs overlapped with DEGs from larval stages (Fig. 3c).
157 Next, we performed GO enrichment tests comparing bPAC+ and bPAC-. Upregulated DEGs
158 in bPAC+ fish brains at 6 dpf were enriched in RNA processing and DNA replication and
159 repair (upper panel of Fig. 3d, S. Table 2). In contrast, downregulated DEGs at 6 dpf were
160 enriched in processes related to nervous system development including neuron differentiation
161 and cell morphogenesis (bottom panel of Fig. 3d, S. Table 2). Indeed, we confirmed alteration
162 of neurogenesis in larval bPAC+ fish[18]. Together these results indicate dysregulation of normal
163 developmental processes in bPAC+ brains in early life coupled with potential genomic
164 instability, replication stress[27], and delayed or immature differentiation of neuronal cells. At
165 120 dpf, despite a smaller numbers of DEGs identified (Fig. 3c), we noted significant
166 upregulation of genes involved in pre-mRNA splicing and 5-hydroxymethyl cytosine (hmC)
167 reading (*wdr76*, *neil1*, and *hells*)[28] suggesting differential epigenetic processes while
168 downregulation of some of the marker genes for oligodendrocyte (*sox10*, *olig2*) indicating
169 decreased oligodendrocyte differentiation in adult bPAC+ brains (S. table 1).
170 Further, we carried out bPAC+ and wild type or bPAC- and wild type comparisons to determine
171 potential effects resulting from high GC exposure that occurred in the bPAC+ parental
172 generation. Even with more stringent thresholds to identify DEGs (FDR < 0.01 and |log2FC| >
173 2) than those of previous comparisons, the upregulated DEGs enriched GO terms in later
174 developmental stages were similar to those identified in the bPAC+ vs. bPAC- comparison
175 including cell cycle, DNA metabolic process, and RNA processing processes (left panel of S.
176 Fig. 2c). Downregulated DEGs across all time points were enriched in processes related to cell
177 adhesion and cell migration, as well as nervous system development including neuron
178 differentiation, cell morphogenesis, and axon development (right panel of S. Fig. 2c), similar
179 to the bPAC+ versus bPAC- comparison. Also, the identified upregulated DEGs in the larval
180 stage of bPAC+ compared to wild type were enriched in potential metabolic enzymes for GC
181 such as cytochrome monooxygenases, 11β-hydroxysteroid dehydrogenase or
182 sulfotransferases[29-31] (left panel of S. Fig. 2c). Some of those DEGs were also significant even
183 in the comparison between bPAC- and wildtype (S. Table 2) suggesting alteration in GC
184 metabolism resulting from elevated GC in parental generation. Lastly, 2.08% (27/1295) and
185 16.6% (211/1259) of up- and downregulated DEGs identified during larval stages in the
186 comparison between bPAC- and wild type overlapped with DEGs identified in the comparison
187 between bPAC+ and bPAC- (Fig. 3e, marked with red double-headed arrows, S. Fig. 2d).
188 However, in adulthood, much fewer overlapping DEGs were identified compared to larval

189 stages (S. Fig. 2d). Together these results identify transcriptional differences caused by dGC
190 exposure and suggest the existence of alterations induced by high GC exposure in the parental
191 generation apparent in both bPAC+ and bPAC-.
192
193 **High GC exposure during development leads to exaggerated transcriptional response to**
194 **acute stress in adulthood**
195 We next examined transcriptional response of bPAC+ upon acute stress exposure in adulthood.
196 To identify a class of genes that are induced by acute stress exposure only in bPAC+, we carried
197 out comparisons by genotype (bPAC+ vs. bPAC-) or condition (pre- vs. post-LD) (Fig. 4a).
198 bPAC+ fish showed a much greater transcriptional response following LD exposure compared
199 to bPAC- fish (Fig. 4b). Strikingly, bPAC+ showed more than 17-fold greater number of DEGs
200 in response to LD exposure (bPAC+ in Fig. 4c, 1754 genes) compared to bPAC- (bPAC- in
201 Fig. 4c, 102 genes). 83% of DEGs induced by LD-exposure in bPAC- were identical to those
202 in bPAC+, while only 17 DEGs were specific to bPAC-. These results indicate that dGC-
203 exposure primed a large number of latent alterations which become only apparent upon acute
204 stress exposure in adulthood in bPAC+ fish. We refer to these differentially regulated genes
205 following LD-exposure in bPAC+ (bPAC+ or bPAC- specific DEGs; 1669 and 17 genes) as
206 developmental GC-primed genes (dGC-primed genes, a total of 1686 genes) (Fig. 4c). dGC-
207 primed genes were significantly overrepresented in the GO terms synapse, cell morphogenesis,
208 regulation of signaling, and more (Fig. 4d-e, S. Table 4), and approximately 80% of dGC-
209 primed genes (1362 genes) were downregulated. For example, synapse associated dGC-primed
210 genes were mostly downregulated and showed enhanced alteration following LD (Fig. 4e).
211 Among the genes associated with GC signaling, we observed that the expression of *nr3c1* (GR)
212 is not altered in bPAC+ adults while the expressions of *nr3c2* (mineralocorticoid receptor; MR)
213 and *crhr1* (corticotropin releasing hormone receptor) were significantly downregulated only in
214 bPAC+ adults following LD exposure (S. Fig. 3a). Moreover, we identified that several key
215 molecules within the CRH signaling pathway were altered in adult bPAC+ brains following
216 LD (S. Fig. 3b), consistent with the observed downregulation of *crhr1* in bPAC+ following LD
217 (S. Fig. 3a).
218
219 **dGC-primed genes are associated with neuropsychiatric disorders in humans**
220 Since ELS is a strong risk factor for developing psychiatric disorders in humans which manifest
221 in adulthood triggered by stressful life events[2-4], we asked whether dGC-primed genes could
222 overlap with psychiatric disease risk factors identified in humans. Remarkably, human

223 homologs of dGC-primed genes exhibit a significant enrichment of known psychiatric disease-
224 associated genes curated in the DisGeNET database[32] (Fig. 4f, S. Table 5). Top-ranked
225 psychiatric disorders were schizophrenia, bipolar disorder, intellectual disability, autistic
226 disorder, and depressive disorder (Fig. 4f-g). In addition, we carried out a comparison with a
227 recent study that reported 702 GC-primed DEGs linked with long-lasting differentially
228 methylated sites following re-exposure to GC (dexamethasone) in a human hippocampal
229 progenitor/neuron cell line[15] and identified 103 genes overlapping with DEGs identified in
230 post-LD bPAC+ vs. post-LD bPAC- comparison (up/down=58/45) and 19 of those were dGC-
231 primed genes (S. Fig. 4, S. Table 6). Notably, some of these post-LD bPAC+ DEGs were
232 already modified at 6 dpf in bPAC+ (transtemporal, 430 DEGs), even though the magnitude of
233 alterations were not always maintained at different stages while some others were altered
234 uniquely in bPAC+ adulthood upon acute stress (adult-onset, 997 DEGs) (Fig. 4h). These
235 results suggest that some dGC-primed genes can be already predicted in early stages following
236 dGC-exposure. Thus, our result identifies a hitherto uncharacterized set of dGC-primed genes
237 that are overrepresented in synapse and cell signaling molecules as well as homologs of human
238 psychiatric disease risk factors.
239
240 **A subset of GC-primed transcriptional alterations is associated with differential DNA**
241 **methylation and alternative splicing patterns in adulthood**
242 To identify potential mechanisms establishing dGC-primed transcriptional alterations, we
243 analyzed expression patterns of DNA methylation modifiers across different time points (S.
244 Fig. 5). Among them, we found a significant difference in the levels of *dnmt3aa* and *dnmt3bb.3*
245 in the bPAC+ fish compared to bPAC- and wild type at 6 dpf (Fig. 5a). The significant
246 difference in *dnmt3aa* level in bPAC+ was maintained into adulthood. Similarly, the level of
247 *tet1,* implicated in demethylation, is altered in bPAC+ adults compared to bPAC- and wildtype
248 after LD exposure (Fig. 5a).
249 To determine whether differential DNA methylation contributes to dGC-primed transcriptional
250 alterations following LD exposure, we identified methylated cytosines (5mCs) in the adult
251 brains of bPAC+ before LD exposure using whole genome sequencing via Oxford nanopore
252 sequencing (S. Fig. 6). Since the majority of dGC-primed genes defined here (1657 genes) are
253 differentially regulated in bPAC+ compared to both wild type and bPAC- (S. Fig. 6a) and
254 previously published reports described transgenerational effects on DNA methylation in
255 zebrafish[33,34], we carried out a comparison of bPAC+ with wildtype brain to identify
256 differentially methylated CpG sites (DMCs). 17.9% of dGC-primed genes (297/1657 genes)

exhibited significant DMCs within their promoter and/or gene body regions (Fig. 5b). Furthermore, we identified a reduced ratio of dGC-primed genes with DMCs in their exonic regions compared to the overall distribution for all DEGs (Fig. 5b). For further analyses, we first focused on the 4937 DMCs which are located within regulatory regions of 64 GC-primed genes (promoter, exon1 and intron1)[35] (S. Table 7). Among them, 2624 and 2313 DMCs on 33 and 31 GC-primed genes showed a negative or correlation between DNA methylation level and gene expression, respectively (Fig. 5c). Although common biological functions encompassing these 64 GC-primed genes were not found, we observed genes associated with gene expression regulators (*dnmt3aa*, *hipk2*, *ccnt1*) as well as top two GO terms in Fig. 4d (synapse and cell morphogenesis; *gphna*, *plxnb2b*, *sema5ba*, and *unc5a*) (Fig. 5c). In addition, we found hypermethylated CpGs on genomic regions associated with dGC-primed genes, *auts2a*, *mapre3a*, *igfbp5a*, *pde4cb*, which overlapped with identified GC-primed DEGs in in vitro dexamethasone treated human neurons[15] (S. Table 7). Overall, these results suggest that altered DNA methylation patterns may associate with establishing of dGC-primed genes in bPAC+ brain.

Lastly, to identify additional mechanisms establishing dGC-primed gene expression, we analyzed the expression pattern of a broader category of epigenetic modifiers in dGC-primed and post-LD DEG gene sets. A total of 48 identified genes were associated with RNA processing including splicing and modification (yellow bar, up/down=18/12), histone modification (dark green bar, up/down=2/13), and DNA methylation modification (purple bar, up/down=0/3) which were altered following LD-exposure in bPAC+ brain (Fig. 5d). 13 genes (corresponding 27%) have at least three significant DMCs on their promoter and gene body regions suggesting a differential regulation mediated by 5mC patterns (Fig. 5e, labeled in red). Strikingly 62% of altered epigenetic modifiers we identified were associated with RNA processing including RNA splicing factors that are involved in U1, U2, or U12-dependent mRNA splicing and RNA-binding proteins that may play important roles in the nervous system[36-41]. Indeed, we identified differential usage of transcript variants between bPAC+ and bPAC- in 64 dGC-primed genes (3.8% of dGC-primed genes, Fig. 5f, S. Table 9, S. Data File 2). The most common and significant alterations in dGC-primed genes were alternative transcription termination sites (ATTSs) and alternative 5'end donor site (A5) (Fig. 5g). Together these results point to DNA methylation and RNA processing as regulatory mechanisms establishing dGC-primed transcriptional alterations.

Discussion

291 We report here that a gene set enriched in the processes of DNA/RNA processing, neuron
292 projection, and neuronal signaling components are altered following dGC-exposure. Strikingly
293 dGC exposure led to exaggerated endocrine stress responses and primed a set of genes to
294 exhibit altered transcriptomic responses to acute stress in adulthood. We identified a
295 comprehensive list of brain-wide dGC-primed gene set and revealed that some of these DEGs
296 are associated with neuropsychiatric disorders in humans and include a set of gene expression
297 modulators. Lastly, we identify DNA methylation and RNA processing as gene regulatory
298 mechanisms that may contribute to establishing of the dGC-primed response to acute stress in
299 adulthood.
300
301 The dGC-primed gene set identified here shares a significant overlap with a previous report of
302 GC-primed genes using neuronal cells derived from human[15]. However, we could only confirm
303 a limited number of overlapping DNA methylation pattern alterations between our study and
304 those identified in the previously published study. DNA methylation patterns and gene
305 expression are known to vary in the tissue/cell type and in a species-specific manner[35,42-44].
306 Given the possible roles and transcriptomic alterations in oligodendrocytes and astrocytes
307 following stress and excess GC[45,46], major differences between our and the previously reported
308 GC-primed genes likely result from differences in the type of samples used namely *in vitro*
309 human neurons versus zebrafish whole-brain samples containing neuronal and non-neuronal
310 cells.
311
312 Interestingly, we identified a large set of upregulated DEGs were enriched in DNA metabolism,
313 various RNA processing processes, and posttranslational modifications as well as epigenetic
314 modifiers including DNA methyltransferases. For example, we have identified a subset of
315 upregulated dGC-primed RNA splicing factors that are involved in U1, U2 or U12-dependent
316 mRNA splicing, including *rbmx2, rbm5, srrm1, rbm25a/b, luc7l,* and *rnpc3*[47-50]. Also, we
317 observed a downregulation of genes encoding dGC-primed RNA-binding proteins, such as
318 *elavl4, qkib, celf2, celf5a, celf5b, nova1,* and *pum2*, which may play important roles in the
319 nervous system[36-41]. Moreover, the most commonly identified transcript variances between
320 bPAC+ vs bPAC- were alternative transcription start sites (ATSSs) and ATTSs. In the context
321 of tissue-dependent exon usage, it was reported that the alternative transcription start and
322 termination sites played an important role[51]. Therefore, the identified ATSSs and ATTSs
323 associated with dGC-primed genes may be regional or cell-type dependent alterations,
324 indicating that dGC-exposure may be able to prime genes in a cell-type or regional-specific

325 manner. Furthermore, alternative donor sites are involved in exon definition[52], repressor-
326 activator competition[53] as well as psychiatric disorders[54,55]. In a similar context, a recent study
327 reported that the administration of dexamethasone, an activator of the GR, also results in
328 alterations to the profile of alternatively spliced genes[56]. Since an increasing body of evidence
329 underscores the role of alternative splicing in diseases including psychiatric disorders[54,57],
330 further studies like using long-read sequencing may reveal an even greater number of
331 alternative splicing events induced by exposure to dGC. Collectively, dGC-exposure may
332 increase the risk of dysregulation of gene expression in the later life stage by disturbing
333 epigenetic regulations and RNA processing in adulthood.
334
335 Our results indicate that LD-exposure alters *nr3c2* (MR) and *crhr1* expression specifically in
336 dGC-exposed animals while the expression of *nr3c1* (GR) is not altered. While GCs can bind
337 both GR and MR in the brain, where many cells express both types of receptors, MR binding
338 typically occurs at low levels of GC concentration, such as during resting state. In contrast, the
339 lower affinity GR is usually occupied only under high GC concentration, such as under stress
340 or at circadian peak[58]. Accordingly, MR and GR operate coordinately in a complementary
341 fashion in response to environmental demands and an imbalance of MR/GR ratio is predicted
342 to compromise the initiation and termination of the stress response leading to HPA axis
343 dysregulation and impaired behavioral adaptation[59-61]. In this regard, it will be interesting to
344 determine the specific site of MR:GR expression imbalance upon LD exposure in our model
345 and assess their potential roles in affected behaviors in bPAC+ animals.
346
347 As early exposure to excess GC is considered a global risk factor for the development of mental
348 disorders, our behavioral pipeline was tailored to assess performance in key behavioral
349 manifestations rather than disease-specific tasks. bPAC+ fish did not show defects in aspects
350 of perception as they can recognize visual and olfactory stimuli in the form of social cues and
351 food pellets. Interestingly, bPAC+ fish exhibited a reduction in the maintenance of social
352 interactions compared to the wild type, but not to bPAC-. We hypothesize that the attenuation
353 of social interactions could potentially be influenced by paternal epigenetic memories resulting
354 from developmental exposure to GCs. These effects should not be underestimated as they could
355 serve as a significant contributory factor to the emergence of divergent social interaction
356 patterns in adulthood. In previous zebrafish ELS studies, diminished shoaling behavior was
357 observed following early-life social isolation and was associated with both motivational
358 deficiencies linked to dopaminergic systems[62] and increased sensitivity to stimuli which was

359 reversed by anxiolytic treatment[63]. Impairments in social behavior or social withdrawal are
360 common among different psychiatric disorders, including autism[64] and schizophrenia[65], and
361 have been described in rodent models of ELS in which deficits in social interaction in the
362 absence of social recognition and approach have been observed[66]. Further, bPAC+ fish showed
363 deficits in fear learning compared to wild type using a Pavlovian conditioning paradigm that
364 pairs electric shock with the color green. It is possible that perceived salience of electric shock
365 as a stressor rather than fear learning is diminished in bPAC+. However, we consider this
366 possibility less likely as bPAC+ can respond robustly to acute stress presented in the form of
367 LD. This phenotype is consistent with what has been reported in rodent ELS models, which
368 showed deficits in fear learning, learning impairment, and decreased cognitive flexibility[67-69].
369 Differences in how zebrafish learn fear association are dependent on whether they are reactive
370 or proactive responders to stress, raising the question of how bPAC+ fish's response fits into
371 that spectrum[70].
372
373 Recently, gene catalogues of neuropsychiatric disease-associated genes following stressful
374 events including early life stress were reported based on gene expression network, eQTLs and
375 GWAS[32,71,72]. The majority of dGC-primed genes which are associated with schizophrenia,
376 bipolar disorder, depressive disorder, and autistic disorder-associated showed an exaggerated
377 transcriptional response to stress in adult bPAC+ brains. Those DEGs were overrepresented in
378 synaptic signaling processes including genes for GABA receptors (*gabrg2*, *gabbr1a*, *gabbr1b*,
379 *gabra1*, *gabra2a*, *gabra4*, *gabrg2*), glutamate receptors and transporter (*grm1b*, *grm3*, *grm5b*,
380 *grik3*, *grin2b*, *slc17a7a*), dopamine receptors (*drd2a*), cholinergic receptor (*chrm2a*), opioid
381 receptor (*pnoca*), and neurexins (*nlgn1*, *nlgn4xb*). In a human study, genetic variants associated
382 with GR-mediated immediate transcript response were able to predict risk for psychiatric
383 disorders including depression[73]. Consistent with this, our findings suggest developmental GC
384 exposure leads to differences in GR-induced transcriptional activation in adult brains and may
385 mediate the risk for psychiatric disorders by altering a network of neuronal signaling-related
386 stress-sensitive genes.
387
388 In conclusion, we identified highly exaggerated transcriptional response in animals with
389 exposure to a high level of GC during development. However, further investigation is required
390 to reveal the consequence of altered epigenetic modulators and a direct mechanistic link
391 between the identified dGC-primed genes and alterations in regulatory mechanisms.

392 We propose that the brain DEG set identified here will be useful for guiding future studies
393 dissecting the mechanisms underlying developmental GC-exposure and alteration of behaviors
394 and neuropsychiatric disease susceptibility in adulthood. The zebrafish model presented here
395 provides an opportunity to dissect the long-term effects of endogenous GC elevation during
396 development and can be leveraged in future studies to identify the critical period, intensity, and
397 duration of developmental GC exposure as well as epigenetic regulatory mechanisms including
398 RNA processing and DNA methylation that leads to adult dysfunction.
399
400 **Methods and materials**
401 The detailed protocol for the generation of transgenic animal, behavioral tests in this study is
402 available as step-wise online methods[74].
403
404 **Zebrafish husbandry and maintenance**
405 The tübingen (TU) strain and transgenic line, *Tg(star:bPAC-2A-tdTomato)*^{uex300} were kept at
406 28°C on a 12:12 hour light/dark cycle and housed at a maximum density of 5 fish/L. For
407 experiments with adult fish, only females were used. All animal procedures were carried out
408 in compliance with the ethical guidelines of the national animal welfare law and approved by
409 relevant authorities (Landesuntersuchungsamt Rheinland-Pfalz, Germany, Project number 23
410 177-07/G20-1-033 or UK Home Office PPL number PEF291C4D).
411
412 **Sample collection**
413 All samples were collected within a 2-hour window in the morning (08:30 to 10:30) without
414 feeding.
415
416 **Whole-body Cortisol assay**
417 The competitive cortisol assay (Cisbio HTRF® Cortisol Kit, 62CRTPEG) was performed
418 following the manufacturer's protocol. ELISA signal was detected by CLARIO star plate
419 reader (BMG Labtech, Ortenberg, Germany).
420
421 **Behavior tests**
422 Social behavior tests and acute stressor delivery using looming dot (LD) presentation were
423 carried out as described in Cook *et al.*[21]. Basal locomotion, food consumption, and fear
424 conditioning assay were performed following the protocol in online methods[74]. For all
425 behavioral tests, female adult zebrafish (6-9 months old) were moved into a designated

426 behavior experimental room one week prior to testing and housed in groups of 10 fish in 3L
427 tanks.
428
429 **RNA preparation and quantification**
430 Each sample for the larval stage (6 and 13 dpf) contained 25-30 larval whole brains whilst for
431 the adult stage (120 dpf) three brains constituted one sample. We dissected the larval whole
432 brains (at 6 or 13 dpf) in the RNAlater® (AM7021, Ambion, USA) after overnight incubation
433 and the adult brains (at 120 dpf) were dissected in PBS on ice and then snap freeze in liquid
434 nitrogen. Samples were kept at -80℃ until further processing. Larval and adult samples were
435 completely homogenized in RNA Lysis buffer from the Quick-RNA miniprep Kit (R1055,
436 Zymo Research, Irvine, CA, USA) using a pestle and micro-tube homogenizer (for 30 sec) or
437 TissueLyser LT (QIAGEN, Dusseldorf, Germany, at 25 Hz for 1 minute and then 15 Hz for 2
438 minutes), respectively. Total RNAs were isolated by following the manufacturer′s protocol and
439 keep it at -80℃ until further use. Transcripts were quantified using real-time qPCR and next-
440 generation mRNA sequencing. cDNA was synthesized using a High-Capacity RNA-to-
441 cDNA™ Kit (4387406, Applied Biosystems, USA) following the manufacturer's protocol. The
442 real-time qPCR was performed with PowerUp™ SYBR™ Green Master Mix (A25778,
443 Applied Biosystems, USA) and specific primers. Primer information for qPCR is described in
444 online methods[74]. mRNA-seq library preparation and sequencing were performed by TRON
445 gGmbH (Mainz, Germany) using the Illumina NovaSeq6000. Briefly, construct paired-end
446 TruSeq Stranded mRNA libraries (Illumina, CA, USA) and sequence it for over 20M of 50 bp
447 reads/sample. A total of 60 samples was sequenced, consisting of 5 biological replicates at four
448 different time points (6, 13, 120 dpf, and acute-stressed at 120 dpf) for each genotype (wild
449 type, bPAC+ and bPAC-).
450
451 **DNA preparation and quantification**
452 Whole brains were collected from 9-month-old bPAC+ and wild type fish. 6 individual brains
453 per group were used for DNA isolation using DNeasy® Blood & Tissue kit (#69504,
454 QIAGENE) following the manufacturer's protocol. Purified DNA was sequenced using the
455 Oxford nanopore sequencing system. Ligation sequencing libraries were prepared from 1000
456 ng DNA using the Ligation Sequencing kit SQK-LSK114 (ONT, Oxford Nanopore
457 Technologies Ltd., Oxford, UK) following the manufacturer's protocol. The clean-up step after

458 adapter ligation was intended to size-select fragments and was done with Long Fragment
459 Buffer. The library was loaded on a single R10.4.1 (FLO-PRO114M) flow cell and sequenced
460 on a PromethION 24 device within 72 h. MinKNOW (v22.12.05) was used to supervise the
461 initial sequencing run.
462
463 **Bioinformatic analyses**
464 mRNA sequencing:
465 RNA sequencing analyses were performed following the online methods[74]. Briefly, processed
466 qualified sequencing reads by FASTQC[75], fastp[76] were mapped to the zebrafish reference
467 genome assembly (GRCz11) with Ensembl annotation version 107 using HISAT[77]. We
468 estimated the expression of transcripts using Stringtie[78] and DEGs using edgeR[79]. Downstream
469 and statistical analyses were performed with in-house R scripts on and Rstudio (Build 485)[80].
470 DEGs were defined with criteria; $|FC| > 1.5$ and $FDR < 0.05$ for the comparisons between
471 bPAC+ vs. bPAC-, or $|FC| > 2$ and $FDR < 0.01$ for the comparisons between bPAC+ vs. wild
472 type. Functional analyses were performed with the R packages including clusterprofiler[81],
473 gProfiler2[82], enrichGO[81] and DisGeNET[32]. Protein-protein interaction networks were
474 constructed and visualized by using the String database[83] and Cytoscap[84]. Alternative splicing
475 and isoform switches were analyzed by using IsoformSwitchAnalyzeR[85].
476
477 Long Read Sequencing:
478 The sequenced reads quality assessment was done using pycoQC[86]. The reads from each
479 sample were base-called using Guppy (v6.4.2, Oxford Nanopore Technologies Ltd) and
480 mapped to the *Danio rerio* (GRCz11) genome using minimap2 aligner[87]. 5mC CpG modified
481 bases were determined using the modbam2bed tool (Oxford Nanopore Technologies Ltd).
482
483 Differential methylation analysis:
484 Differential methylation analysis between control and stress samples was done using DSS
485 Bioconductor package[88] with $p < 0.05$. Bases were considered as differentially methylated if
486 $FDR < 0.05$ and absolute DNA methylation difference between two groups larger than 25%.
487
488 Genomic coordinates of exon, intron, promoter, and intergenic region for *Danio rerio* genome
489 were obtained from the UCSC genome browser. Promoters were defined as upstream 800bps
490 and downstream 200bps from TSS. Differentially methylated cytosines were annotated based
491 on genomic positions into exons, introns, promoters, and intergenic regions using the Genomic

Ranges findOverlaps function[89]. Methylation browser tracks were created using deeptools bamCoverage utility[90]. The variant calling was performed using Clair3 package[91].

Code availability

The detailed data processing and R scripts for bioinformatic analysis are available at the GitHub repository (https://github.com/minkechoi/tx_star-bPAC_brain).

Data availability

All sequenced reads for RNA-seq were deposited in European Nucleotide Archive (ENA, PRJEB53713).

Statistics

Statistical analyses were performed using R and Prism 9 (Graphpad Software Inc, San Diego, CA, USA). A detailed description of the statistical analyses is provided in online methods[74]

Acknowledgment

This project was funded by the German Federal Office for Education and Research (BMBF) grant number 01GQ1404 and Mireille and Dennis Gillings Foundation Grant to SR, Basic Science Research Program (2020R1A6A3A03037828) of National Research Foundation (NRF) of Korea to MC and Institutional Strategic Support Fund 3 scheme (ISSF3) to Translational Research Exchange @ Exeter (ISSF3-TREE-Choi, 2022) funded by Wellcome Trust to MC. We acknowledge the support of TRON gGmbH (Mainz, Germany) for the RNA-sequencing, Aquatic Resources Center (University of Exeter, UK), and Kathrin Domdera (University of Mainz, DE) for expert fish care, and High-Performance Computing (HPC) facility (University of Exeter, UK) for the server for informatic analyses.

Author contributions

SR conceived the project. MC and SR designed the project. MC acquired and analyzed omics data. KM and ML generated and analyzed ONT-seq data. AC acquired and analyzed behavior data. HE, and AT contributed to reagent generation or data acquisition. MC, SR, and AC drafted the article. MC, HE, and SR critically revised the manuscript. All authors approved the submission.

Competing interests

SR holds a patent, European patent number 2928288 and US patent number 10,080,355: “A novel inducible model of stress.”. The remaining authors declare no known competing interests.

Figure legends

Figure 1. Double-hit stress model shows elevation of cortisol during development and upon acute stress exposure in adulthood. (a) A scheme illustrating the strategy for underlying Double-hit zebrafish stress model which combines *i)* optogenetic cortisol elevation during development and *ii)* adulthood acute stress exposure. Arrows indicate sample collection times points. (b) An image of *Tg(star:bPAC-2A-tdTomato)*$^{+/-}$ larva at 5 dpf. The transgene is expressed solely in the interrenal gland (arrow). A schematic drawing representing the intracellular events within the steroidogenic interrenal cells of the transgenic fish (dotted box). Endogenous GC production is stimulated by ACTH signaling. bPAC mimics ACTH signaling by increasing cAMP when exposed to blue light. (c) One of the well-known GR signaling markers, *fkbp5*, was significantly upregulated in bPAC+ larvae compared to bPAC- and wildtype control. ** = $P<0.01$. Tukey's multiple comparisons test following one-way ANOVA, F (2, 6) = 16.25, $P=0.0038$. (d-e) Basal cortisol level at larval stages and from juvenile to adult. (f) Schematic of the acute stress paradigm. Looming dots mimic approaching predators from above (Cook *et al*. 2023). Total 10 times of LD were given as an acute stress. (g) bPAC+ showed significantly higher cortisol levels following LD, compared to handling controls (no LD presented on the screen). Tukey's multiple comparisons following one-way ANOVA; F(5, 54)=19.31, $P<0.0001$. Abbreviations: dpf: day post fertilization, mpf: month post fertilization, GC: glucocorticoid, ACTH: Adrenocorticotropic Hormone, AC: adenylyl cyclase, cAMP: Cyclic adenosine monophosphate, FC: fold change, LD: Looming dots, wt: wild type, ctrl: control, bPAC: *beggiatoa* photoactivated adenylyl cyclase.

Figure 2. Altered behaviors in adult bPAC+, bPAC- and wildtype fish. (a) A schematic depicting experimental groups. (b-c) No significant differences were observed in average speed nor turn frequency among wild type, bPAC+ and bPAC-. Dunnett's multiple comparisons followed one-way ANOVA, b) F(2, 27)=0.2248, $P=0.80$; c) F(2, 27)=2.332, $P=0.12$. (d) A schematic drawing for the novel tank test. (e) Average depth as measured by average distance from the bottom of tank was greater for wild type and bPAC- compared to bPAC+. (f-g) bPAC+ fish showed a slower average speed than wild type and reduced fast swimming bouts compared to bPAC- and wild type. (h) A schematic for the feeding behavior test. (i-j) bPAC+ significantly consumed fewer number of pellets within 10 min compared to wild type or bPAC-. (k) bPAC+ spent more time near the food compared to wildtype or bPAC-. (l) Schematic figures for the social approach and maintenance test. (m) Representative traces of wild-type, bPAC+ and bPAC- when conspecifics are visible. The green shaded area indicates the interaction zone where wildtype fish typically spent most of their time when conspecifics are visible. (n-o) During this social phase, bPAC+ and bPAC- showed a significantly reduced duration and frequency of social interactions compared to the wild type (Cook rt al., 2023}. (p) A schematic drawing for a chamber used for the fear conditioning test. (q) An electric shock was given to subject fish when they swim in the green colored area. After conditioning, time spent in each color zone was measured. (r) No significant difference was observed in color preference prior to fear conditioning. (s) bPAC+ showed less preference for the safe zone color (blue) after the conditioning using an electric shock. Error bars on bar graphs indicate the mean±SD and shading in line graphs represents the mean±SEM. Tukey's multiple comparisons followed one-way ANOVA. f) F(2, 33)=7.806, $P=0.002$; g) F(2, 33)=17.31, $P<0.0001$; j) F(2, 37)=8.364, $P=0.001$; k) F(2, 36) = 9.120, $P<0.001$, n) F(2, 98)=6.273, $P=0.0027$; o) F(2, 98)=10.93, $P<0.0001$; s) F(2, 45)=8.927, $P<0.001$.

Figure 3. Developmental GC exposure leads to differential gene expressions across the life course. (a) Read counts of genes by genotype and time points are represented by z-score in the heat map. Bars on the left side indicate the genotype of fish (yellow: bPAC+, green:

bPAC-, dark purple: wild type) and time points (gray: 6 dpf, dark gray: 13 dpf, black: 120 dpf). (b) Volcano plot showing DEGs (red dots) in bPAC+ and bPAC- brain transcriptome at 6 dpf. Dashed lines indicate FDR and FC cut-off values set at 0.05 and 1.5, respectively. Labels identify the genes associated with cortisol or circadian rhythm among the smallest FDR values. Plots for other time points are available in the Supplementary data file. Complete list of identified DEGs described in S. Table 1. (c) Venn Diagram for up- and down-regulated DEGs among wild type, bPAC- and bPAC+; criteria for DEG identification: |FC|>1.5 and FDR <0.05. (d) Top enriched GO terms for up- and down-regulated DEGs in bPAC+ compared to bPAC- at 6 dpf. Complete list of DEG-enriched GO terms are described in S. Table 2. (e) Circos plots showing overlapping DEGs by linked line among three pairwise comparisons, bPAC+ vs. bPAC-, bPAC+ vs. wild type, bPAC- vs. wild type. FDR: False discovery rate, GO: Gene ontology, *adj.p*: adjusted *P*-value.

Figure 4. Developmental GC exposure primes differential gene expression following acute stress in bPAC+ adults. (a) Venn diagram representing DEGs between bPAC+ and bPAC- in pre-LD and post-LD conditions. (b) Schematic for three comparisons to identify transcriptional changes in response to LD exposure in adults. DEGs were determined by FC and FDR. |FC|>1.5 and FDR<0.05. (c) Venn diagram showing post-LD DEGs from bPAC+ and bPAC-. The list of DEGs is described in S. Table 3. dGC-primed genes are marked by dashed line. (d) The top GO terms enriched in dGC-primed genes. The enrichment score = $-\log_{10}$(adjusted *P*-value). (e) PPI networks of synapse associated dGC-primed genes. The size of node indicates fold-change. Networks sourced by STRING. (f) Result of human disorders enrichment test based on the DisGeNET database using GC-primed genes. The ratio represents overlapping/input genes. Top ranked disorders are Schizophrenia (FDR= 1.12e-04, ratio=122/883), Bipolar Disorder (FDR= 2.47e-03, ratio=69/477), Intellectual Disability (FDR= 1.71e-02, ratio=61/447), Autistic Disorder (FDR= 1.87e-04, ratio=48/261), Depressive disorder (FDR= 4.51e-03, ratio=46/289), and Mental Depression (FDR= 4.06e-03, ratio=42/254). The complete results are noted in S. Table 5. (g) Venn diagram for dGC-primed genes that are associated with the top human psychiatric disorders in panel f. (h) Heatmap showing log2FC of 2174 LD-DEGs across time points demonstrated 430 trans-temporal and 997 adult-onset genes were mostly downregulated. LD: looming dots, FC: fold change, FDR: False discovery rate, PPI: Protein-protein interaction, ratio: GC-primed genes/disease genes, Depressive + MD: Depressive disorder and Mental Depression.

Figure 5. Subsets of GC-primed genes are differentially methylated and spliced in bPAC+ brains. (a) Expression trajectories for differentially expressed *dnmt*s in bPAC+ brains. Šídák's multiple comparisons test followed mixed model ANOVA. The asterisks indicates the time points with significant differential expressions (*adj.P* <0.05 and |FC| >1.5). *dnmt3aa*: $F(6, 39) = 13.13$, $P<0.0001$; *dnmt3bb.3*: $F(6, 39) = 11.26$, $P<0.0001$; *tet1*: $F(6, 39) = 7.037$, $P<0.0001$. (b) The bar graph depicts the number of DEGs exhibiting statistically significant differences in DNA methylation levels, specifically on CpG sites, within both their promoter and gene body regions. (c) Methylation levels of DMCs on the regulatory regions of genes including promoter, exon1, and intron1 were positively or negatively correlated with subsets of GC-primed genes. (d) Bar graph showing known epigenetic regulators associated with DNA (purple, 3), RNA (yellow, 30), and histone (dark green, 15) modification or process among dGC-primed genes and post-LD DEGs. (e) Heatmap represents $\log_2$FC of them. The asterisk in each cell refers to FDR < 0.05. Red label indicates existence of DMCs on their corresponding regions. (f) Summary of identified alternative splicing events between bPAC+ vs. bPAC-. (g) Enrichment test of alternative splicing events. ES: Exon Skipping, MEE: Mutually Exclusive Exon, MES: Multiple Exon Skipping, IR: Intron Retention, A5: Alternative 5'end donor site,

A3: Alternative 3'end acceptor site, ATSS: Alternative Transcription Start Sites, ATTS: Alternative Transcription Termination Sites.

632 **References**

633 1 Brunson, K. L. *et al.* Mechanisms of late-onset cognitive decline after early-life stress.
634 *J Neurosci* **25**, 9328-9338 (2005). https://doi.org:10.1523/jneurosci.2281-05.2005
635 2 Kessler, R. C. *et al.* Childhood adversities and adult psychopathology in the WHO
636 World Mental Health Surveys. *Br J Psychiatry* **197**, 378-385 (2010).
637 https://doi.org:10.1192/bjp.bp.110.080499
638 3 McEwen, B. S. & Gianaros, P. J. Central role of the brain in stress and adaptation:
639 links to socioeconomic status, health, and disease. *Ann N Y Acad Sci* **1186**, 190-222
640 (2010). https://doi.org:10.1111/j.1749-6632.2009.05331.x
641 4 Heim, C. & Nemeroff, C. B. The role of childhood trauma in the neurobiology of
642 mood and anxiety disorders: preclinical and clinical studies. *Biol Psychiatry* **49**, 1023-
643 1039 (2001). https://doi.org:10.1016/s0006-3223(01)01157-x
644 5 Peña, C. J. *et al.* Early life stress confers lifelong stress susceptibility in mice via
645 ventral tegmental area OTX2. *Science* **356**, 1185-1188 (2017).
646 https://doi.org:doi:10.1126/science.aan4491
647 6 Balouek, J.-A. *et al.* Reactivation of Early-Life Stress-Sensitive Neuronal Ensembles
648 Contributes to Lifelong Stress Hypersensitivity. *The Journal of Neuroscience* **43**, 5996-
649 6009 (2023). https://doi.org:10.1523/jneurosci.0016-23.2023
650 7 McLaughlin, K. A. *et al.* Childhood social environment, emotional reactivity to stress,
651 and mood and anxiety disorders across the life course. *Depression and Anxiety* **27**,
652 1087-1094 (2010). https://doi.org:https://doi.org/10.1002/da.20762
653 8 Chyu, L. & Saxton, K. Early life adversity increases the salience of later life stress: an
654 investigation of interactive effects in the PSID. *Journal of Developmental Origins of*
655 *Health and Disease* **11**, 25-36 (2020). https://doi.org:10.1017/S2040174419000308
656 9 Charmandari, E., Tsigos, C. & Chrousos, G. Endocrinology of the stress response.
657 *Annu Rev Physiol* **67**, 259-284 (2005).
658 https://doi.org:10.1146/annurev.physiol.67.040403.120816
659 10 Wendelaar Bonga, S. E. The stress response in fish. *Physiol Rev* **77**, 591-625 (1997).
660 https://doi.org:10.1152/physrev.1997.77.3.591
661 11 Lupien, S. J., McEwen, B. S., Gunnar, M. R. & Heim, C. Effects of stress throughout
662 the lifespan on the brain, behaviour and cognition. *Nat Rev Neurosci* **10**, 434-445
663 (2009). https://doi.org:10.1038/nrn2639
664 12 Vidrascu, E. M., Bashore, A. C., Howard, T. D. & Moore, J. B. Effects of early- and mid-
665 life stress on DNA methylation of genes associated with subclinical cardiovascular
666 disease and cognitive impairment: a systematic review. *BMC Medical Genetics* **20**, 39
667 (2019). https://doi.org:10.1186/s12881-019-0764-4
668 13 Weaver, I. C. *et al.* Epigenetic programming by maternal behavior. *Nat Neurosci* **7**,
669 847-854 (2004). https://doi.org:10.1038/nn1276
670 14 Peña, C. J. *et al.* Early life stress alters transcriptomic patterning across reward
671 circuitry in male and female mice. *Nat Commun* **10**, 5098 (2019).
672 https://doi.org:10.1038/s41467-019-13085-6
673 15 Provençal, N. *et al.* Glucocorticoid exposure during hippocampal neurogenesis
674 primes future stress response by inducing changes in DNA methylation. *Proc Natl*
675 *Acad Sci U S A* **117**, 23280-23285 (2020). https://doi.org:10.1073/pnas.1820842116
676 16 Gutierrez-Triana, J. A. *et al.* Manipulation of Interrenal Cell Function in Developing
677 Zebrafish Using Genetically Targeted Ablation and an Optogenetic Tool.
678 *Endocrinology* **156**, 3394-3401 (2015). https://doi.org:10.1210/en.2015-1021

17 Nagpal, J., Eachus, H., Lityagina, O. & Ryu, S. Optogenetic induction of chronic glucocorticoid exposure in early-life impairs stress-response in larval zebrafish. *bioRxiv*, 2022.2009.2009.507267 (2022). https://doi.org:10.1101/2022.09.09.507267

18 Eachus, H. *et al.* Elevated Glucocorticoid alters the trajectory of hypothalamic development and function. *bioRxiv*, 2023.2001.2027.525966 (2023). https://doi.org:10.1101/2023.01.27.525966

19 Bali, U., Phillips, T., Hunt, H. & Unitt, J. FKBP5 mRNA Expression Is a Biomarker for GR Antagonism. *The Journal of Clinical Endocrinology & Metabolism* **101**, 4305-4312 (2016). https://doi.org:10.1210/jc.2016-1624

20 Scharf, S. H., Liebl, C., Binder, E. B., Schmidt, M. V. & Müller, M. B. Expression and regulation of the Fkbp5 gene in the adult mouse brain. *PLoS One* **6**, e16883 (2011). https://doi.org:10.1371/journal.pone.0016883

21 Cook, A., Beckmann, H., Azap, R. & Ryu, S. Acute stress modulates social approach and social maintenance in adult zebrafish. *bioRxiv*, 2023.2002.2010.528021 (2023). https://doi.org:10.1101/2023.02.10.528021

22 Egan, R. J. *et al.* Understanding behavioral and physiological phenotypes of stress and anxiety in zebrafish. *Behavioural Brain Research* **205**, 38-44 (2009). https://doi.org:https://doi.org/10.1016/j.bbr.2009.06.022

23 Cachat, J. M. *et al.* in *Zebrafish Neurobehavioral Protocols* (eds Allan V. Kalueff & Jonathan M. Cachat) 1-14 (Humana Press, 2011).

24 Kenney, J. W., Scott, I. C., Josselyn, S. A. & Frankland, P. W. Contextual fear conditioning in zebrafish. *Learning & Memory* **24**, 516-523 (2017). https://doi.org:10.1101/lm.045690.117

25 Brock, A. J., Sudwarts, A., Daggett, J., Parker, M. O. & Brennan, C. H. A fully automated computer-based 'Skinner Box' for testing learning and memory in zebrafish. *bioRxiv*, 110478 (2017). https://doi.org:10.1101/110478

26 Theodoridi, A. *et al.* Knockout of the hsd11b2 Gene Extends the Cortisol Stress Response in Both Zebrafish Larvae and Adults. *Int J Mol Sci* **22** (2021). https://doi.org:10.3390/ijms222212525

27 Zheng, D.-Q., Zhang, K., Wu, X.-C., Mieczkowski, P. A. & Petes, T. D. Global analysis of genomic instability caused by DNA replication stress in Saccharomyces cerevisiae. *Proceedings of the National Academy of Sciences* **113**, E8114-E8121 (2016). https://doi.org:doi:10.1073/pnas.1618129113

28 Spruijt, Cornelia G. *et al.* Dynamic Readers for 5-(Hydroxy)Methylcytosine and Its Oxidized Derivatives. *Cell* **152**, 1146-1159 (2013). https://doi.org:https://doi.org/10.1016/j.cell.2013.02.004

29 Gulliver, L. S. Xenobiotics and the Glucocorticoid Receptor. *Toxicol Appl Pharmacol* **319**, 69-79 (2017). https://doi.org:10.1016/j.taap.2017.02.003

30 Draper, N. & Stewart, P. M. 11beta-hydroxysteroid dehydrogenase and the pre-receptor regulation of corticosteroid hormone action. *J Endocrinol* **186**, 251-271 (2005). https://doi.org:10.1677/joe.1.06019

31 Balyan, R. *et al.* Repeated restraint stress upregulates rat sulfotransferase 1A1. **30**, 265-273 (2019). https://doi.org:doi:10.1515/jbcpp-2016-0038

32 Piñero, J., Saüch, J., Sanz, F. & Furlong, L. I. The DisGeNET cytoscape app: Exploring and visualizing disease genomics data. *Computational and Structural Biotechnology Journal* **19**, 2960-2967 (2021). https://doi.org:https://doi.org/10.1016/j.csbj.2021.05.015

33 Jiang, L. *et al.* Sperm, but Not Oocyte, DNA Methylome Is Inherited by Zebrafish Early Embryos. *Cell* **153**, 773-784 (2013). https://doi.org:https://doi.org/10.1016/j.cell.2013.04.041

34 Terrazas-Salgado, L. *et al.* Epigenetic Transgenerational Modifications Induced by Xenobiotic Exposure in Zebrafish. *Frontiers in Cell and Developmental Biology* **10** (2022). https://doi.org:10.3389/fcell.2022.832982

35 Anastasiadi, D., Esteve-Codina, A. & Piferrer, F. Consistent inverse correlation between DNA methylation of the first intron and gene expression across tissues and species. *Epigenetics & Chromatin* **11**, 37 (2018). https://doi.org:10.1186/s13072-018-0205-1

36 Ratti, A. *et al.* Post-transcriptional Regulation of Neuro-oncological Ventral Antigen 1 by the Neuronal RNA-binding Proteins ELAV*. *Journal of Biological Chemistry* **283**, 7531-7541 (2008). https://doi.org:https://doi.org/10.1074/jbc.M706082200

37 Zhu, H., Hasman, R. A., Barron, V. A., Luo, G. & Lou, H. A Nuclear Function of Hu Proteins as Neuron-specific Alternative RNA Processing Regulators. *Molecular Biology of the Cell* **17**, 5105-5114 (2006). https://doi.org:10.1091/mbc.e06-02-0099

38 Åberg, K., Saetre, P., Jareborg, N. & Jazin, E. Human QKI, a potential regulator of mRNA expression of human oligodendrocyte-related genes involved in schizophrenia. *Proceedings of the National Academy of Sciences* **103**, 7482-7487 (2006). https://doi.org:doi:10.1073/pnas.0601213103

39 Loria, P. M., Duke, A., Rand, J. B. & Hobert, O. Two Neuronal, Nuclear-Localized RNA Binding Proteins Involved in Synaptic Transmission. *Current Biology* **13**, 1317-1323 (2003). https://doi.org:https://doi.org/10.1016/S0960-9822(03)00532-3

40 Ule, J. *et al.* Nova regulates brain-specific splicing to shape the synapse. *Nature Genetics* **37**, 844-852 (2005). https://doi.org:10.1038/ng1610

41 Martínez, J. C. *et al.* Pum2 Shapes the Transcriptome in Developing Axons through Retention of Target mRNAs in the Cell Body. *Neuron* **104**, 931-946.e935 (2019). https://doi.org:10.1016/j.neuron.2019.08.035

42 Klughammer, J. *et al.* Comparative analysis of genome-scale, base-resolution DNA methylation profiles across 580 animal species. *Nature Communications* **14**, 232 (2023). https://doi.org:10.1038/s41467-022-34828-y

43 Wan, J. *et al.* Characterization of tissue-specific differential DNA methylation suggests distinct modes of positive and negative gene expression regulation. *BMC Genomics* **16**, 49 (2015). https://doi.org:10.1186/s12864-015-1271-4

44 Lokk, K. *et al.* DNA methylome profiling of human tissues identifies global and tissue-specific methylation patterns. *Genome Biology* **15**, 3248 (2014). https://doi.org:10.1186/gb-2014-15-4-r54

45 Cathomas, F. *et al.* Oligodendrocyte gene expression is reduced by and influences effects of chronic social stress in mice. *Genes, Brain and Behavior* **18**, e12475 (2019). https://doi.org:https://doi.org/10.1111/gbb.12475

46 Murphy-Royal, C., Gordon, G. R. & Bains, J. S. Stress-induced structural and functional modifications of astrocytes-Further implicating glia in the central response to stress. *Glia* **67**, 1806-1820 (2019). https://doi.org:10.1002/glia.23610

47 Bai, R. *et al.* Structure of the activated human minor spliceosome. *Science* **371**, eabg0879 (2021). https://doi.org:doi:10.1126/science.abg0879

48 McCracken, S., Longman, D., Johnstone, I. L., Cáceres, J. F. & Blencowe, B. J. An Evolutionarily Conserved Role for SRm160 in 3′-End Processing That Functions

Independently of Exon Junction Complex Formation*. *Journal of Biological Chemistry* **278**, 44153-44160 (2003). https://doi.org:https://doi.org/10.1074/jbc.M306856200

49 Zhou, A., Ou, A. C., Cho, A., Benz, E. J. & Huang, S.-C. Novel Splicing Factor RBM25 Modulates Bcl-x Pre-mRNA 5′ Splice Site Selection. *Molecular and Cellular Biology* **28**, 5924-5936 (2008). https://doi.org:10.1128/MCB.00560-08

50 Argente, J. *et al.* Defective minor spliceosome mRNA processing results in isolated familial growth hormone deficiency. *EMBO Molecular Medicine* **6**, 299-306 (2014). https://doi.org:https://doi.org/10.1002/emmm.201303573

51 Reyes, A. & Huber, W. Alternative start and termination sites of transcription drive most transcript isoform differences across human tissues. *Nucleic Acids Research* **46**, 582-592 (2017). https://doi.org:10.1093/nar/gkx1165

52 Izquierdo, J. M. *et al.* Regulation of Fas Alternative Splicing by Antagonistic Effects of TIA-1 and PTB on Exon Definition. *Molecular Cell* **19**, 475-484 (2005). https://doi.org:10.1016/j.molcel.2005.06.015

53 Zahler, A. M., Damgaard, C. K., Kjems, J. & Caputi, M. SC35 and Heterogeneous Nuclear Ribonucleoprotein A/B Proteins Bind to a Juxtaposed Exonic Splicing Enhancer/Exonic Splicing Silencer Element to Regulate HIV-1 tat Exon 2 Splicing *. *Journal of Biological Chemistry* **279**, 10077-10084 (2004). https://doi.org:10.1074/jbc.M312743200

54 Reble, E., Dineen, A. & Barr, C. L. The contribution of alternative splicing to genetic risk for psychiatric disorders. *Genes, Brain and Behavior* **17**, e12430 (2018). https://doi.org:https://doi.org/10.1111/gbb.12430

55 Kuan, P.-F. *et al.* Mapping the transcriptomics landscape of post-traumatic stress disorder symptom dimensions in World Trade Center responders. *Translational Psychiatry* **11**, 310 (2021). https://doi.org:10.1038/s41398-021-01431-6

56 Magomedova, L. *et al.* ARGLU1 is a transcriptional coactivator and splicing regulator important for stress hormone signaling and development. *Nucleic Acids Research* **47**, 2856-2870 (2019). https://doi.org:10.1093/nar/gkz010

57 Jiang, W. & Chen, L. Alternative splicing: Human disease and quantitative analysis from high-throughput sequencing. *Computational and Structural Biotechnology Journal* **19**, 183-195 (2021). https://doi.org:https://doi.org/10.1016/j.csbj.2020.12.009

58 Reul, J. M., van den Bosch, F. R. & de Kloet, E. R. Differential response of type I and type II corticosteroid receptors to changes in plasma steroid level and circadian rhythmicity. *Neuroendocrinology* **45**, 407-412 (1987). https://doi.org:10.1159/000124766

59 de Kloet, E. R., Joëls, M. & Holsboer, F. Stress and the brain: from adaptation to disease. *Nature Reviews Neuroscience* **6**, 463-475 (2005). https://doi.org:10.1038/nrn1683

60 De Kloet, E. R. *et al.* Plasticity and function of brain corticosteroid receptors during aging. *Acta Endocrinol (Copenh)* **125 Suppl 1**, 65-72 (1991).

61 de Kloet, E. R. From Receptor Balance to Rational Glucocorticoid Therapy. *Endocrinology* **155**, 2754-2769 (2014). https://doi.org:10.1210/en.2014-1048

62 Shams, S., Amlani, S., Buske, C., Chatterjee, D. & Gerlai, R. Developmental social isolation affects adult behavior, social interaction, and dopamine metabolite levels in zebrafish. *Developmental Psychobiology* **60**, 43-56 (2018). https://doi.org:https://doi.org/10.1002/dev.21581

63 Tunbak, H., Vazquez-Prada, M., Ryan, T. M., Kampff, A. R. & Dreosti, E. Whole-brain mapping of socially isolated zebrafish reveals that lonely fish are not loners. *Elife* **9**, e55863 (2020). https://doi.org:10.7554/eLife.55863

64 Chevallier, C., Kohls, G., Troiani, V., Brodkin, E. S. & Schultz, R. T. The social motivation theory of autism. *Trends in Cognitive Sciences* **16**, 231-239 (2012). https://doi.org:https://doi.org/10.1016/j.tics.2012.02.007

65 Miyakawa, T. *et al.* Conditional calcineurin knockout mice exhibit multiple abnormal behaviors related to schizophrenia. *Proceedings of the National Academy of Sciences* **100**, 8987-8992 (2003). https://doi.org:10.1073/pnas.1432926100

66 Todeschin, A. S. *et al.* Effects of neonatal handling on social memory, social interaction, and number of oxytocin and vasopressin neurons in rats. *Hormones and Behavior* **56**, 93-100 (2009). https://doi.org:https://doi.org/10.1016/j.yhbeh.2009.03.006

67 Lehmann, J., Pryce, C. R., Bettschen, D. & Feldon, J. The maternal separation paradigm and adult emotionality and cognition in male and female Wistar rats. *Pharmacol Biochem Behav* **64**, 705-715 (1999). https://doi.org:10.1016/s0091-3057(99)00150-1

68 Aisa, B., Tordera, R., Lasheras, B., Del Río, J. & Ramírez, M. J. Effects of maternal separation on hypothalamic-pituitary-adrenal responses, cognition and vulnerability to stress in adult female rats. *Neuroscience* **154**, 1218-1226 (2008). https://doi.org:10.1016/j.neuroscience.2008.05.011

69 Thomas, A. W., Caporale, N., Wu, C. & Wilbrecht, L. Early maternal separation impacts cognitive flexibility at the age of first independence in mice. *Dev Cogn Neurosci* **18**, 49-56 (2016). https://doi.org:10.1016/j.dcn.2015.09.005

70 Baker, M. R. & Wong, R. Y. Contextual fear learning and memory differ between stress coping styles in zebrafish. *Sci Rep* **9**, 9935 (2019). https://doi.org:10.1038/s41598-019-46319-0

71 Penner-Goeke, S. *et al.* High-throughput screening of glucocorticoid-induced enhancer activity reveals mechanisms of stress-related psychiatric disorders. *Proceedings of the National Academy of Sciences* **120**, e2305773120 (2023). https://doi.org:doi:10.1073/pnas.2305773120

72 Arcego, D. M. *et al.* A Glucocorticoid-Sensitive Hippocampal Gene Network Moderates the Impact of Early-Life Adversity on Mental Health Outcomes. *Biological Psychiatry* **95**, 48-61 (2024). https://doi.org:10.1016/j.biopsych.2023.06.028

73 Arloth, J. *et al.* Genetic Differences in the Immediate Transcriptome Response to Stress Predict Risk-Related Brain Function and Psychiatric Disorders. *Neuron* **86**, 1189-1202 (2015). https://doi.org:https://doi.org/10.1016/j.neuron.2015.05.034

74 Choi, M. *et al.* Comprehensive analysis methods for developmental GC exposed zebrafish. *protocols.io* (2023). https://doi.org:10.17504/protocols.io.kxygx9ooog8j/v3

75 Andrews, S. FASTQC. <https://www.bioinformatics.babraham.ac.uk/projects/fastqc>.

76 Chen, S., Zhou, Y., Chen, Y. & Gu, J. fastp: an ultra-fast all-in-one FASTQ preprocessor. *Bioinformatics* **34**, i884-i890 (2018). https://doi.org:10.1093/bioinformatics/bty560

77 Kim, D., Langmead, B. & Salzberg, S. L. HISAT: a fast spliced aligner with low memory requirements. *Nat Methods* **12**, 357-360 (2015). https://doi.org:10.1038/nmeth.3317

78 Pertea, M., Kim, D., Pertea, G. M., Leek, J. T. & Salzberg, S. L. Transcript-level expression analysis of RNA-seq experiments with HISAT, StringTie and Ballgown. *Nature Protocols* **11**, 1650-1667 (2016). https://doi.org:10.1038/nprot.2016.095

79 Robinson, M. D., McCarthy, D. J. & Smyth, G. K. edgeR: a Bioconductor package for differential expression analysis of digital gene expression data. *Bioinformatics* **26**, 139-140 (2010). https://doi.org:10.1093/bioinformatics/btp616

80 Team, R. RStudio: Integrated Development for R. (2020).

81 Wu, T. *et al.* clusterProfiler 4.0: A universal enrichment tool for interpreting omics data. *The Innovation* **2**, 100141 (2021). https://doi.org:https://doi.org/10.1016/j.xinn.2021.100141

82 Raudvere, U. *et al.* g:Profiler: a web server for functional enrichment analysis and conversions of gene lists (2019 update). *Nucleic Acids Research* **47**, W191-W198 (2019). https://doi.org:10.1093/nar/gkz369

83 Szklarczyk, D. *et al.* STRING v11: protein–protein association networks with increased coverage, supporting functional discovery in genome-wide experimental datasets. *Nucleic Acids Research* **47**, D607-D613 (2019). https://doi.org:10.1093/nar/gky1131

84 Shannon, P. *et al.* Cytoscape: a software environment for integrated models of biomolecular interaction networks. *Genome Res* **13**, 2498-2504 (2003). https://doi.org:10.1101/gr.1239303

85 Vitting-Seerup, K. & Sandelin, A. IsoformSwitchAnalyzeR: analysis of changes in genome-wide patterns of alternative splicing and its functional consequences. *Bioinformatics* **35**, 4469-4471 (2019). https://doi.org:10.1093/bioinformatics/btz247

86 Leger, A. & Leonardi, T. pycoQC, interactive quality control for Oxford Nanopore Sequencing. *Journal of Open Source Software* **4** (2019). https://doi.org:10.21105/joss.01236

87 Li, H. Minimap2: pairwise alignment for nucleotide sequences. *Bioinformatics* **34**, 3094-3100 (2018). https://doi.org:10.1093/bioinformatics/bty191

88 Feng, H. & Wu, H. Differential methylation analysis for bisulfite sequencing using DSS. *Quant Biol* **7**, 327-334 (2019). https://doi.org:10.1007/s40484-019-0183-8

89 Lawrence, M. *et al.* Software for Computing and Annotating Genomic Ranges. *PLOS Computational Biology* **9**, e1003118 (2013). https://doi.org:10.1371/journal.pcbi.1003118

90 Ramírez, F. *et al.* deepTools2: a next generation web server for deep-sequencing data analysis. *Nucleic Acids Research* **44**, W160-W165 (2016). https://doi.org:10.1093/nar/gkw257

91 Zheng, Z. *et al.* Symphonizing pileup and full-alignment for deep learning-based long-read variant calling. *Nature Computational Science* **2**, 797-803 (2022). https://doi.org:10.1038/s43588-022-00387-x

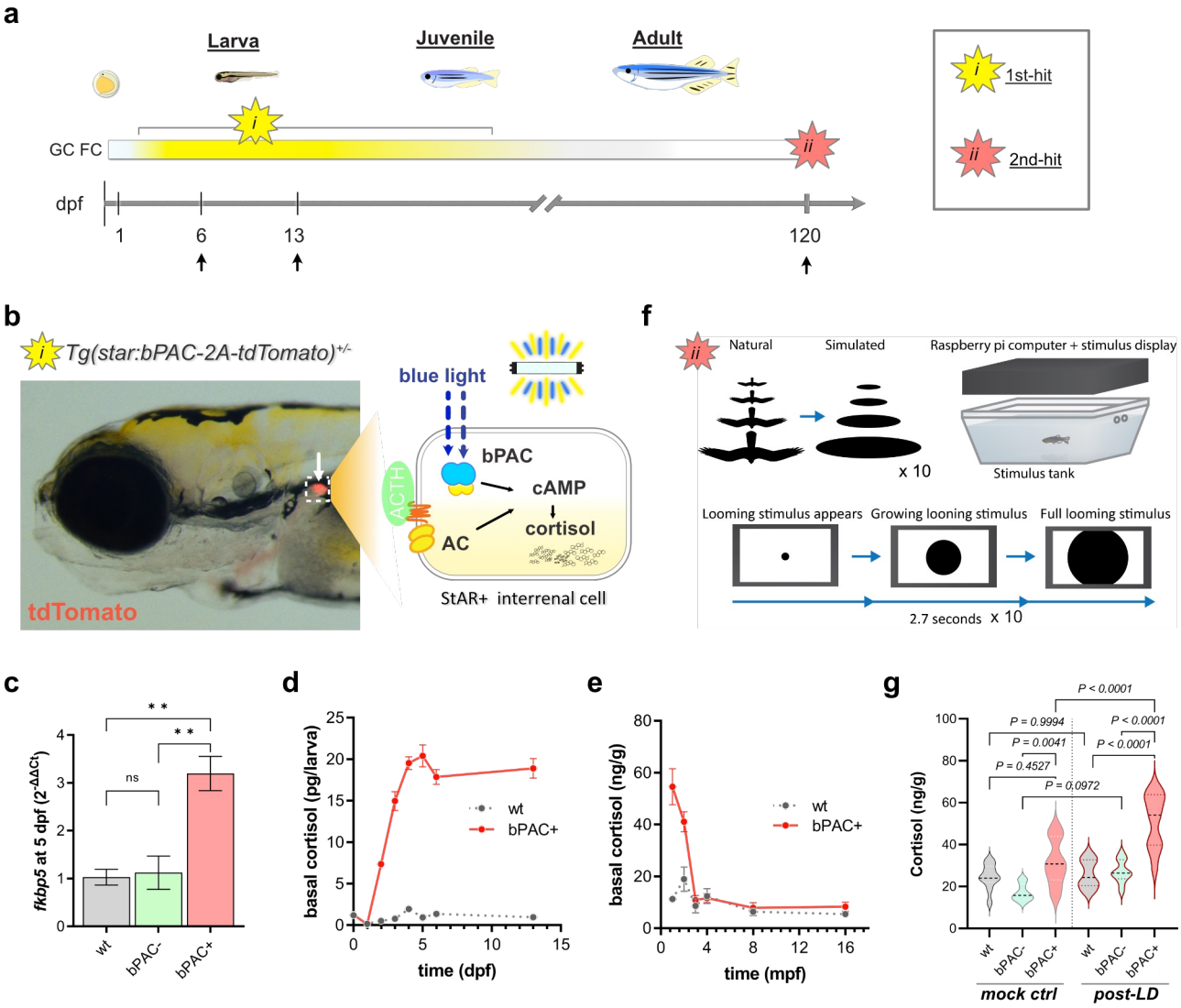
a
Larva
Juvenile
Adult
GC FC
dpf
1
6
13
120
1st-hit
2nd-hit
b
Tg(star:bPAC-2A-tdTomato)+/-
tdTomato
blue light
bPAC
cAMP
cortisol
AC
ACTH
StAR+ interrenal cell
f
Natural
Simulated
Raspberry pi computer + stimulus display
x 10
Stimulus tank
Looming stimulus appears
Growing looning stimulus
Full looming stimulus
2.7 seconds x 10
c
fkbp5 at 5 dpf (2-ΔΔCt)
ns
wt
bPAC-
bPAC+
d
basal cortisol (pg/larva)
time (dpf)
wt
bPAC+
e
basal cortisol (ng/g)
time (mpf)
wt
bPAC+
g
Cortisol (ng/g)
P < 0.0001
P = 0.9994
P < 0.0001
P = 0.0041
P < 0.0001
P = 0.4527
P = 0.0972
mock ctrl
post-LD

Figure 1

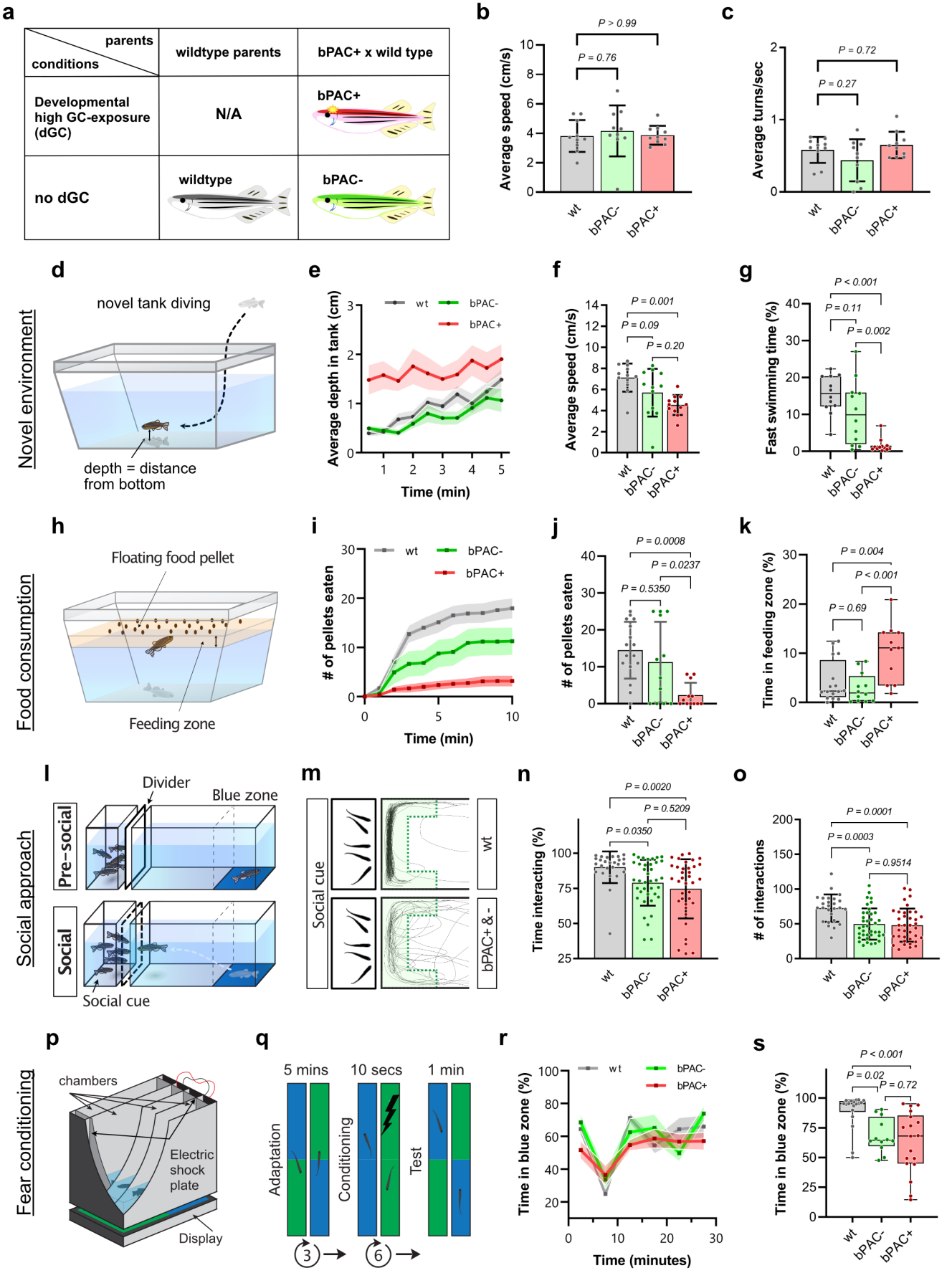
a
parents
conditions
wildtype parents
bPAC+ x wild type
Developmental high GC-exposure (dGC)
N/A
bPAC+
no dGC
wildtype
bPAC-
b
Average speed (cm/s)
P > 0.99
P = 0.76
wt
bPAC-
bPAC+
c
Average turns/sec
P = 0.72
P = 0.27
Novel environment
d
novel tank diving
depth = distance from bottom
e
Average depth in tank (cm)
Time (min)
f
Average speed (cm/s)
P = 0.001
P = 0.09
P = 0.20
g
Fast swimming time (%)
P < 0.001
P = 0.11
P = 0.002
Food consumption
h
Floating food pellet
Feeding zone
i
# of pellets eaten
Time (min)
j
# of pellets eaten
P = 0.0008
P = 0.0237
P = 0.5350
k
Time in feeding zone (%)
P = 0.004
P < 0.001
P = 0.69
Social approach
l
Divider
Blue zone
Pre-social
Social
Social cue
m
Social cue
wt
bPAC+ & -
n
Time interacting (%)
P = 0.0020
P = 0.5209
P = 0.0350
o
# of interactions
P = 0.0001
P = 0.0003
P = 0.9514
Fear conditioning
p
chambers
Electric shock plate
Display
q
5 mins
10 secs
1 min
Adaptation
Conditioning
Test
r
Time in blue zone (%)
Time (minutes)
s
Time in blue zone (%)
P < 0.001
P = 0.02
P = 0.72

Figure 2

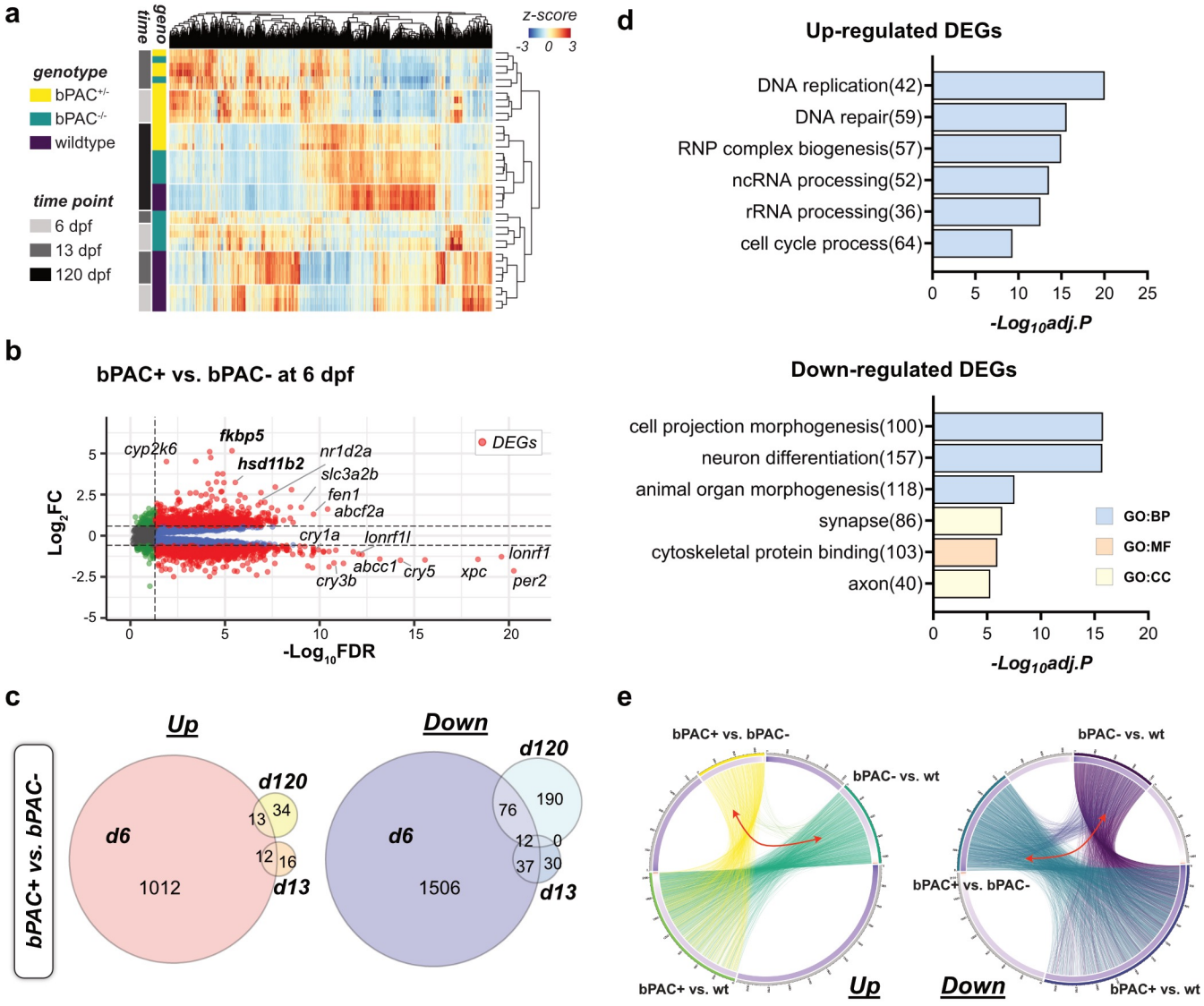
a
geno
time
z-score
-3 0 3
genotype
bPAC+/-
bPAC-/-
wildtype
time point
6 dpf
13 dpf
120 dpf
b
bPAC+ vs. bPAC- at 6 dpf
DEGs
cyp2k6
fkbp5
hsd11b2
nr1d2a
slc3a2b
fen1
abcf2a
cry1a
lonrf1l
lonrf1
abcc1
cry5
xpc
cry3b
per2
Log2FC
-Log10FDR
c
bPAC+ vs. bPAC-
Up
Down
d6
d120
d13
1012
34
13
12
16
1506
190
76
12
0
37
30
d
Up-regulated DEGs
DNA replication(42)
DNA repair(59)
RNP complex biogenesis(57)
ncRNA processing(52)
rRNA processing(36)
cell cycle process(64)
-Log10adj.P
Down-regulated DEGs
cell projection morphogenesis(100)
neuron differentiation(157)
animal organ morphogenesis(118)
synapse(86)
cytoskeletal protein binding(103)
axon(40)
GO:BP
GO:MF
GO:CC
-Log10adj.P
e
bPAC+ vs. bPAC-
bPAC- vs. wt
bPAC+ vs. wt
Up
bPAC- vs. wt
bPAC+ vs. bPAC-
bPAC+ vs. wt
Down

Figure 3

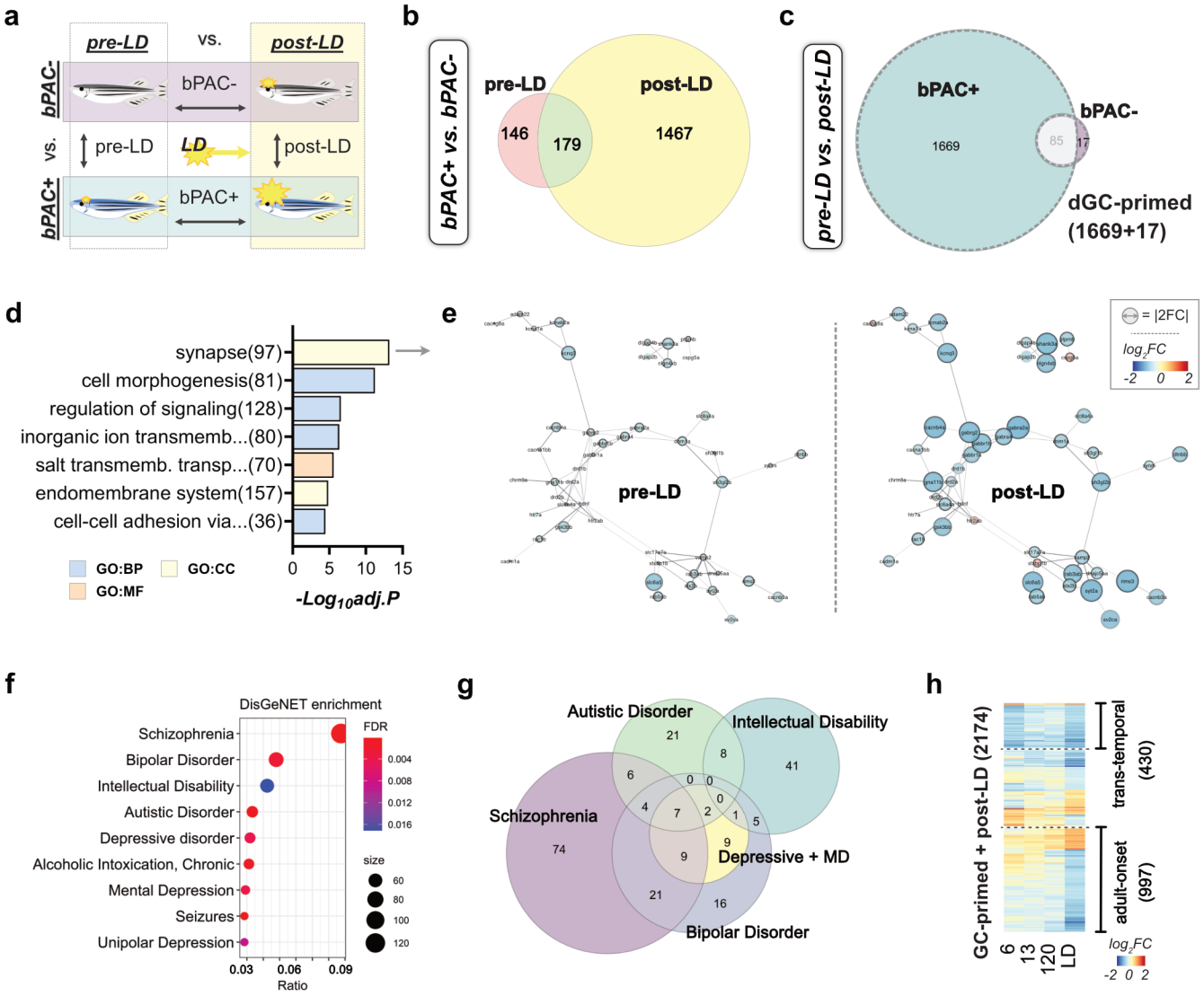
a
pre-LD
vs.
post-LD
bPAC-
bPAC-
vs.
pre-LD
LD
post-LD
bPAC+
bPAC+
b
bPAC+ vs. bPAC-
pre-LD
post-LD
146
179
1467
c
pre-LD vs. post-LD
bPAC+
1669
85
17
bPAC-
dGC-primed
(1669+17)
d
synapse(97)
cell morphogenesis(81)
regulation of signaling(128)
inorganic ion transmemb...(80)
salt transmemb. transp...(70)
endomembrane system(157)
cell-cell adhesion via...(36)
GO:BP
GO:CC
GO:MF
0
5
10
15
-Log10adj.P
e
pre-LD
post-LD
= |2FC|
log2FC
-2
0
2
f
DisGeNET enrichment
Schizophrenia
Bipolar Disorder
Intellectual Disability
Autistic Disorder
Depressive disorder
Alcoholic Intoxication, Chronic
Mental Depression
Seizures
Unipolar Depression
FDR
0.004
0.008
0.012
0.016
size
60
80
100
120
0.03
0.06
0.09
Ratio
g
Autistic Disorder
Intellectual Disability
Schizophrenia
Depressive + MD
Bipolar Disorder
21
8
41
6
0
0
0
4
7
2
1
5
74
9
9
21
16
h
GC-primed + post-LD (2174)
trans-temporal
(430)
adult-onset
(997)
6
13
120
LD
log2FC
-2
0
2

Figure 4

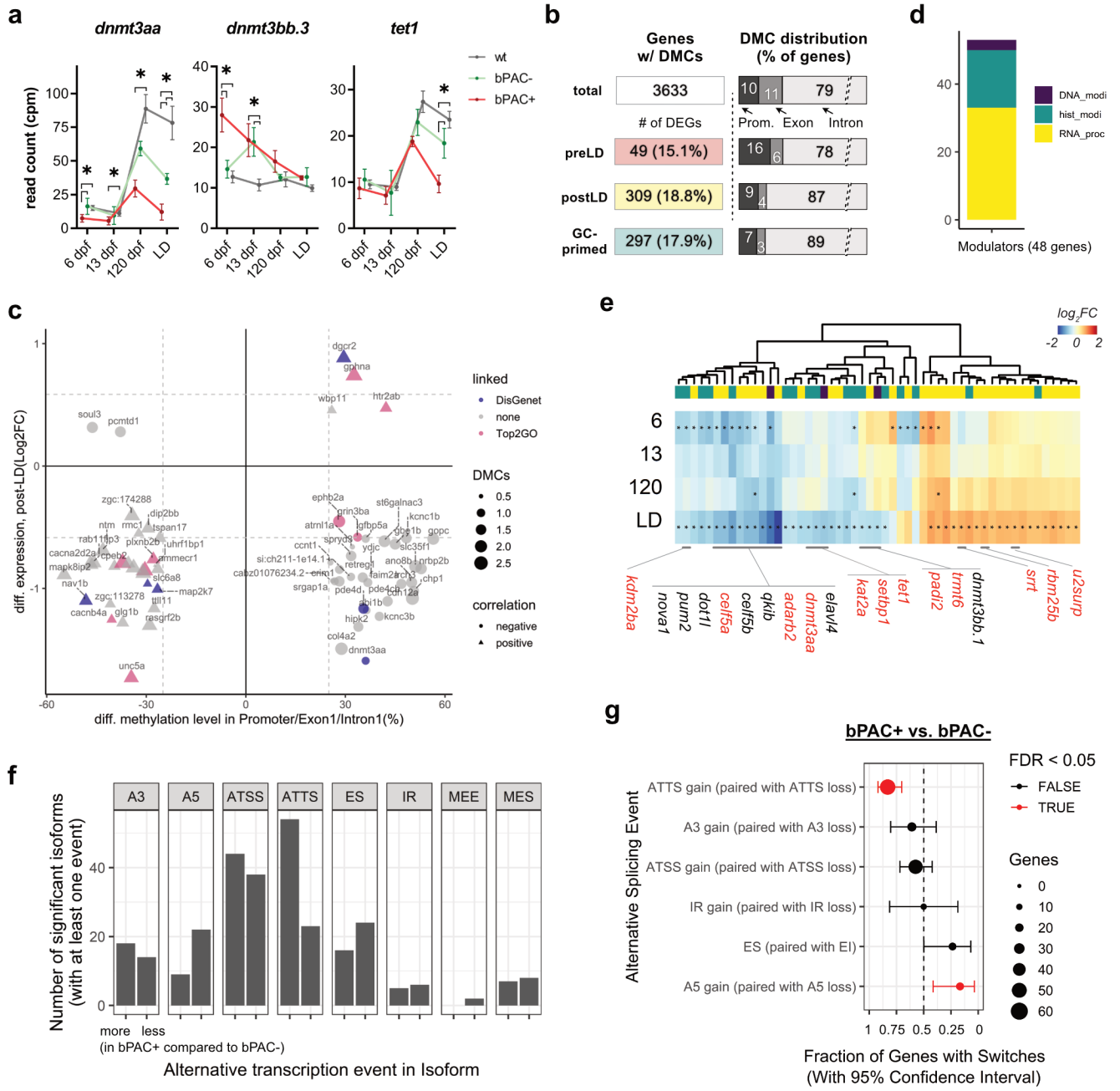
a
dnmt3aa
dnmt3bb.3
tet1
read count (cpm)
wt
bPAC-
bPAC+
6 dpf
13 dpf
120 dpf
LD
b
Genes w/ DMCs
DMC distribution (% of genes)
total
3633
# of DEGs
Prom.
Exon
Intron
preLD
49 (15.1%)
postLD
309 (18.8%)
GC-primed
297 (17.9%)
d
DNA_modi
hist_modi
RNA_proc
Modulators (48 genes)
c
diff. expression, post-LD(Log2FC)
diff. methylation level in Promoter/Exon1/Intron1(%)
linked
DisGenet
none
Top2GO
DMCs
correlation
negative
positive
e
log2FC
6
13
120
LD
kdm2ba
nova1
pum2
dot1l
celf5a
celf5b
qkib
adarb2
dnmt3aa
elavl4
kat2a
setbp1
tet1
padi2
trmt6
dnmt3bb.1
srt
rbm25b
u2surp
f
A3
A5
ATSS
ATTS
ES
IR
MEE
MES
Number of significant isoforms (with at least one event)
more
less
(in bPAC+ compared to bPAC-)
Alternative transcription event in Isoform
g
bPAC+ vs. bPAC-
FDR < 0.05
FALSE
TRUE
Genes
Alternative Splicing Event
ATTS gain (paired with ATTS loss)
A3 gain (paired with A3 loss)
ATSS gain (paired with ATSS loss)
IR gain (paired with IR loss)
ES (paired with EI)
A5 gain (paired with A5 loss)
Fraction of Genes with Switches
(With 95% Confidence Interval)

Figure 5